Numerical results for Saito's uniqueness theorem in inverse scattering theory

Teemu Tyni

Department of Mathematics and Statistics

University of Helsinki, Finland

Abstract

We consider an inverse scattering problem for the Schrödinger operator in two dimensions. The aim of this work is to discuss some first numerical results on Saito's formula. Saito's formula is an explicit integral formula, which at the high-frequency limit gives a uniqueness result for the inverse scattering problem. The numeric approach is quite straight-forward: we take a large enough fixed wave number and evaluate the integrals in Saito's formula numerically. The potential function can then be recovered from the blurry measurements by using the fast Fourier transform and a high-pass filter. We also discuss in detail how the synthetic data is generated via a matrix-based approach. Several numerical examples are shown to demonstrate the results.

1   Introduction

This paper is concerned with an inverse scattering problem for the time-independent Schrödinger operator

$$Hu := -\Delta u + Vu, \quad \text{in } \mathbb{R}^2, \tag{1}$$

where $\Delta = \frac{\mathrm{d}^2}{\mathrm{d}x_1^2} + \frac{\mathrm{d}^2}{\mathrm{d}x_2^2}$ is the Laplace operator in $\mathbb{R}^2$ and where the potential function V belongs to a suitable function space. In scattering theory, one often considers the equation

$$Hu = k^2 u, \quad u = u_0 + u_{\mathrm{sc}}, \quad u_0(x, k, \theta) = \mathrm{e}^{\mathrm{i}k\langle \mathbf{x}, \theta \rangle}, \tag{2}$$

where $k > 0$ is the wave number, u_0 is the incoming plane wave with incident direction $\theta \in \mathbb{S}^1 := \{\mathbf{x} \in \mathbb{R}^2 \mid |\mathbf{x}| = 1\}$ and u_{sc} is the outgoing scattered field. Here $\langle \cdot, \cdot \rangle$ denotes the usual inner product in $\mathbb{R}^2$. The scattered field is required to satisfy the following Sommerfeld's radiation condition (see e.g., [3, 28]) at infinity:

$$\lim_{|\mathbf{x}| \to \infty} |\mathbf{x}|^{\frac{1}{2}} \left(\langle \mathbf{x}/|\mathbf{x}|, \nabla u_{\mathrm{sc}} \rangle - \mathrm{i}k u_{\mathrm{sc}} \right) = 0,$$

uniformly to all directions $\mathbf{x}/|\mathbf{x}| =: \theta' \in \mathbb{S}^1$, where the symbol ∇ denotes the gradient. We mention also that there exists a Besov space characterization of the radiation condition, see for example [14]. Under the radiation condition there exists a unique solution to (2) and this solution can be equivalently obtained as the unique solution to the Lippmann-Schwinger integral equation

$$u(\mathbf{x}, k, \theta) = u_0(\mathbf{x}, k, \theta) - \int_{\mathbb{R}^2} G_k^+(|\mathbf{x} - \mathbf{y}|) V(\mathbf{y}) u(\mathbf{y}, k, \theta) \mathrm{d}\mathbf{y}. \tag{3}$$

Here G_k^+ is the kernel of the integral operator $(-\Delta - k^2 - \mathrm{i}0)^{-1}$. This kernel is a radiating fundamental solution to the differential operator $-\Delta - k^2$, that is, it satisfies the radiation condition at infinity and $(-\Delta - k^2)G_k^+ = \delta$ in the sense of distributions.

In scattering theory one is interested in measurements far away from the scatterer. This asymptotic behaviour of the solution u at $|\mathbf{x}| \to +\infty$ is given by

$$u(\mathbf{x}, k, \theta) = u_0(\mathbf{x}, k, \theta) - \frac{1 + \mathrm{i}}{4\sqrt{\pi}} \frac{\mathrm{e}^{\mathrm{i}k|\mathbf{x}|}}{\sqrt{k|\mathbf{x}|}} A(k, \theta, \theta') + o\left(\frac{1}{\sqrt{|\mathbf{x}|}}\right), \tag{4}$$

where $\theta' = \mathbf{x}/|\mathbf{x}| \in \mathbb{S}^1$ is the measurement direction. The function $A(k, \theta, \theta')$ is called the scattering amplitude and it is defined by

$$A(k, \theta, \theta') = \int_{\mathbb{R}^2} \mathrm{e}^{-\mathrm{i}k\langle\theta', \mathbf{y}\rangle} V(\mathbf{y}) u(\mathbf{y}, k, \theta) \mathrm{d}\mathbf{y}.$$

Before diving deeper into Saito's formula, let us mention some previous numerical results in the spirit of this paper. In acoustic tomography, de Hoop et al. [11] studied a fixed energy problem. They showed how to recover an unknown potential from the Dirichlet-to-Neumann map using the so-called D-bar method, which is based on the exponentially growing complex geometric optics solutions, and developed methods to solve the required boundary integral equations. Research has also been done on the fixed energy problem for the Schrödinger operator, for which Fotopoulos, Harju and Serov [8, 26] used a Born approximation of the so-called scattering transform to reconstruct the unknown potential function. For multi-frequency measurements, numerically the inverse Born approximation is very effective [9]. It is simply the Fourier transform of the scattering amplitude in the frequency domain and can be used for instance with backscattering data, i.e. when the measurement direction $\theta' = -\theta$ and with fixed angle data where θ or θ' is kept constant, see e.g. [7]. We mention also the recent results [15, 16, 17], where inverse scattering for the Helmholtz equation is considered. Their approach is based on a convexification of the Dirichlet-to-Neumann map and the methods are tested on synthetic and experimental data sets.

2

In 1982 Y. Saitō [22] showed that for a three-dimensional close-range potential V the following limit holds:

$$\lim_{k \to \infty} k^2 \int_{\mathbb{S}^2 \times \mathbb{S}^2} e^{-ik\langle \theta - \theta', \mathbf{x} \rangle} A(k, \theta, \theta') \mathrm{d}\theta \mathrm{d}\theta' = C \int_{\mathbb{R}^3} \frac{V(\mathbf{y})}{|\mathbf{x} - \mathbf{y}|^2} \mathrm{d}\mathbf{y}.$$

Since then, this formula has been generalized to all dimensions $n \geq 2$ [21] with more general, possibly nonlinear, potentials V [23, 25] and in some cases with different operators H [30]. In this work our attention is on the two-dimensional result

$$\lim_{k \to \infty} k \int_{\mathbb{S}^1 \times \mathbb{S}^1} e^{-ik\langle \theta - \theta', \mathbf{x} \rangle} A(k, \theta, \theta') \mathrm{d}\theta \mathrm{d}\theta' = 4\pi \int_{\mathbb{R}^2} \frac{V(\mathbf{y})}{|\mathbf{x} - \mathbf{y}|} \mathrm{d}\mathbf{y}. \tag{5}$$

Provided that V is sufficiently integrable, for example $V \in L^p_{2\delta}(\mathbb{R}^2)$, where $2 < p \leq \infty$ and $\delta > 1 - \frac{1}{p}$, Saito's formula holds uniformly in $\mathbf{x} \in \mathbb{R}^2$. Here $L^p_\delta(\mathbb{R}^2)$ is the weighted Lebesgue space defined by the norm $\|f\|_{L^p_\delta(\mathbb{R}^2)} := \|(1 + |\mathbf{x}|^2)^{\delta/2} f\|_{L^p(\mathbb{R}^2)}$. Furthermore, the right-hand side of formula (5) defines a bounded function. Since the right-hand side is equal to zero (in the sense of distributions) only when $V \equiv 0$ we obtain the following uniqueness result.

Theorem 1.1. *Let $V_1, V_2 \in L^p_{2\delta}(\mathbb{R}^2)$, where $2 < p \leq \infty$ and $\delta > 1 - \frac{1}{p}$. If the corresponding scattering amplitudes $A_1(k_j, \theta, \theta')$ and $A_2(k_j, \theta, \theta')$ are equal for some sequence $k_j \to +\infty$ and for all directions $\theta, \theta' \in \mathbb{S}^1$, then the potentials V_1 and V_2 are equal almost everywhere.*

Remark 1.2. In this work we do not consider the rate of convergence in Saito's formula. In our numerical experiments, taking $k \geq 10$ yields reasonable reconstructions: see Section 4 for more.

From numerics point of view the difficulty of using Saito's formula for inverse scattering problems arises from number of oscillatory integrals: it can be difficult to even obtain the synthetic data. The approach we take in this text is to compute the scattered field only inside the support of V, which we will assume is compact, and then use

$$A(k, \theta, \theta') = \int_{\mathbb{R}^2} e^{-ik\langle \theta', \mathbf{y} \rangle} V(\mathbf{y}) u(\mathbf{y}, k, \theta) \mathrm{d}\mathbf{y} = \mathcal{F}[Vu(\cdot, k, \theta)](k\theta'). \tag{6}$$

The benefit of this point of view is that one has only to calculate u within the support of V, where G_k^+ behaves nicely with respect to oscillations so that Vu is not too badly oscillating. So if we can compute the required oscillatory Fourier integral, we can obtain our simulated measurements. Highly oscillatory integrals of Fourier-type have been researched thoroughly and many algorithms exist for their numerical

evaluation. We mention here the works of Evans and Webster [4, 5], Iserles [12, 13], Levin [20], and Shampine [27].

This paper is organized as follows. We start in Section 2 by generating the simulated measurements. This is done by solving the Lippmann-Schwinger equation inside the support of V and then taking the Fourier transform of Vu. In Section 3 we first compute the integral of Saito's formula over incident and measurement directions numerically. We then give a simple fast Fourier transform based filtering method to invert Saito's formula. Finally, in Section 4 we show several numerical examples which demonstrate the recovery of the shape, location and size of the potential V.

2   Simulating the scattering amplitude

Let us denote the integral operator appearing in the Lippmann-Schwinger equation by L_k, that is,

$$u(\mathbf{x}, k, \theta) = u_0(\mathbf{x}, k, \theta) - \int_{\mathbb{R}^2} G_k^+(|\mathbf{x} - \mathbf{y}|)V(\mathbf{y})u(\mathbf{y}, k, \theta)\mathrm{d}\mathbf{y}$$

$$=: u_0 + L_k u. \tag{7}$$

It follows from Agmon's estimates (see Appendix A of [1]) that if $\delta > 1/2$ the resolvent

$$(-\Delta - k^2 - \mathrm{i}0)^{-1} : L_\delta^2(\mathbb{R}^n) \to L_{-\delta}^2(\mathbb{R}^n)$$

is a bounded operator (in the uniform operator topology) which satisfies good norm estimates:

$$\|(-\Delta - k^2 - \mathrm{i}0)f\|_{L_{-\delta}^2(\mathbb{R}^2)} \leq \frac{C_0}{k}\|f\|_{L_\delta^2(\mathbb{R}^2)} \tag{8}$$

for some constant C_0 which only depends on δ. Using this fact, the solution u to (3) can be obtained as the Neumann series in $L_{-2\delta}^2(\mathbb{R}^2)$:

$$u = \sum_{j=0}^{\infty} u_j = \sum_{j=0}^{\infty} L_k^j u_0,$$

provided that $k > k_0$ is sufficiently large. Here

$$u_j(\mathbf{x}, k, \theta) := -\int_{\mathbb{R}^2} G_k^+(|\mathbf{x} - \mathbf{y}|)V(\mathbf{y})u_{j-1}(\mathbf{y}, k, \theta)\mathrm{d}\mathbf{y}, \quad j = 1, 2, \ldots$$

and $u_0(\mathbf{x}, k, \theta) = \mathrm{e}^{\mathrm{i}k\langle\mathbf{x}, \theta\rangle}$. For our purposes it is sufficient to have the solution u on the support of V. In particular, if the support K of V is compact, we have that

4

the operator L_k defined in (7) is compact on $L^2(K)$ and it satisfies the estimate (8) with some different constant.

In some past works on scattering problems with farfield data [6, 9, 29] the approach has been to compute the solution

$$u(\mathbf{x}, k, \theta) \approx u_0(\mathbf{x}, k, \theta) - \int_{\mathbb{R}^2} G_k^+(|\mathbf{x} - \mathbf{y}|) V(\mathbf{y}) \sum_{j=0}^{M} u_j(\mathbf{y}, k, \theta) \mathrm{d}\mathbf{y}.$$

The downside to this approach is that one has to compute the integrals iteratively with, for example, Simpson's rule and Kress rectangular rule [18, 19], which is computationally expensive. Also the large value of the wave number k poses difficulties, since

$$G_k^+(|\mathbf{x} - \mathbf{y}|) = \frac{\mathrm{i}}{4} H_0^{(1)}(k|\mathbf{x} - \mathbf{y}|) \approx \frac{(1 + \mathrm{i})}{4\sqrt{\pi}} \frac{\mathrm{e}^{\mathrm{i}k|\mathbf{x} - \mathbf{y}|}}{\sqrt{k|\mathbf{x} - \mathbf{y}|}},$$

where $H_0^{(1)}$ is the Hankel function of the first kind. If V is compactly supported and the measurements are made far away, at e.g., $\mathbf{x} = R\theta'$ for some $\theta' \in \mathbb{S}^1$ and $R > 0$ large, we see that the kernel is both small in size and oscillatory as $\mathbf{y}$ varies in the support. In any case, this approach would give the scattering amplitude directly, since from (4) we can solve

$$A(k, \theta, \theta') \approx (-2 + 2\mathrm{i})\sqrt{\pi k R} \mathrm{e}^{-\mathrm{i}kR}(u(R\theta', k, \theta) - u_0(R\theta', k, \theta)).$$

In this work we calculate the scattering amplitude as a Fourier transform

$$A(k, \theta, \theta') = \int_{\mathbb{R}^2} \mathrm{e}^{-\mathrm{i}k\langle\theta', \mathbf{y}\rangle} V(\mathbf{y}) u(\mathbf{y}, k, \theta) \mathrm{d}y = \mathcal{F}(V u(\cdot, k, \theta))(k\theta').$$

This way, if the potential function V is compactly supported, it suffices to evaluate the solution of (2) (or equivalently of (3)) just inside $\mathrm{supp}(V)$.

Our approach is a modification of Vainikko's method to solving the Lippmann-Schwinger equation [31]. In essence, Vainikko substitutes instead of G_k^+, V and u in the Lippmann-Schwinger equation their piecewise constant approximations and obtains a linear system

$$u(\mathbf{x}_j, k, \theta) = u_0(\mathbf{x}_j, k, \theta) - h^2 \sum_{i=1}^{m} G_k^+(\mathbf{x}_j - \mathbf{x}_i) V(\mathbf{x}_i) u(\mathbf{x}_i, k, \theta),$$

where h is the step length of the discretization. In [31] also the convergence of this algorithm is studied as $h \to 0$. This will be also our viewpoint, but instead of the piecewise constant approximation of $G_k^+(\mathbf{x}_j - \mathbf{x}_i) V(\mathbf{x}_i)$ we take it's integral over $\mathbf{x}_i$ inside the ith pixel. Consider a grid of m pixels

$$R_j = [x_j - h/2, x_j + h/2] \times [y_j - h/2, y_j + h/2], \quad j = 1, \dots, m,$$

5

of width and height h, containing the support of V. Let χ_A denote the characteristic function of a set $A \subset \mathbb{R}^2$, that is,

$$\chi_A(\mathbf{x}) = \begin{cases} 1, & \text{if } \mathbf{x} \in A, \\ 0, & \text{if } \mathbf{x} \notin A. \end{cases} \tag{9}$$

For brevity, let $\chi_j := \chi_{R_j}$, $j = 1, \ldots, m$, denote the characteristic function of each pixel. We then replace u by a piecewise constant approximation

$$u \approx \sum_{j=1}^{m} \alpha_j \chi_j,$$

where α_j is the value of u at the center $\mathbf{x}_j = (x_j, y_j)$ of the jth pixel. This way we obtain the approximation

$$L_k u(\mathbf{x}_i) \approx L_k \left(\sum_{j=1}^{m} \alpha_j \chi_j \right) (\mathbf{x}_i)$$

$$=: \mathcal{L}_i \overline{\alpha},$$

where $\mathcal{L}_i$ is the ith row of $\mathcal{L}_{ij} = L_k(\chi_j)(\mathbf{x}_i) \in \mathbb{C}^{m \times m}$ and $\overline{\alpha} = (\alpha_1, \ldots, \alpha_m)$.

Here one has to calculate the integrals

$$L_k(\chi_j)(\mathbf{x}_i) = - \int_{\mathbb{R}^2} G_k^+(|\mathbf{x}_i - \mathbf{y}|) V(\mathbf{y}) \chi_j(\mathbf{y}) \mathrm{d}\mathbf{y}$$

at each point $\mathbf{x}_i$ over each pixel R_j. The small size of the pixels helps, since it restricts oscillations of G_k^+. The kernel G_k^+ has a logarithmic singularity along the diagonal $\mathbf{x} = y$, so we need to separate the integration to two cases: we use Simpson's $2n+1$-point quadrature rule outside of the diagonal $i \neq j$ and the Kress rectangular rule [18, 19] on the diagonal $i = j$. The Kress quadrature is of the form

$$\int_0^1 f(x)\mathrm{d}x \approx \sum_{j=1}^{n-1} w_j f(x_j), \quad w_j = \frac{2\pi}{n} w'\left(\frac{2\pi j}{n}\right), \quad x_j = w\left(\frac{2\pi j}{n}\right)$$

and it is suited for integrals with end-point singularities. If the singularity occurs at some other point $c \in]0, 1[$, we can adapt to the intervals $[0, c]$ and $[c, 1]$ instead. Here we choose to use the weight function

$$w(t) = \frac{t^p}{t^p - (2\pi - t)^p}, \quad p = 3.$$

Having computed the matrix $\mathcal{L}$, the values α_j of u can be solved from

$$\overline{\alpha} = \overline{\alpha}_{\text{in}} + \mathcal{L}\overline{\alpha},$$

6

where $\overline{\alpha}_{\mathrm{in}}$ contains the piecewise constant approximation of u_0. One can choose to solve the arising linear system directly and in principle have $\overline{\alpha} = (I - \mathcal{L})^{-1}\overline{\alpha}_{\mathrm{in}}$. A faster, more robust way is to calculate few iterations of the Neumann series

$$\overline{\alpha} = \sum_{j=0}^{\infty} \mathcal{L}^j \overline{\alpha}_{\mathrm{in}}.$$

The convergence of this series follows from the mapping properties of the operator L_k. In our examples (described in Section 4) the matrix norm of $\mathcal{L}$ is close to 0.05, depending on the example. We use $\overline{\alpha} \approx \sum_{j=0}^{5} \mathcal{L}^j \overline{\alpha}_{\mathrm{in}}$. This way we obtain the solution to (3) inside the support of V as a function of $\mathbf{x}$.

Remark 2.1. The matrix $\mathcal{L}$ does not depend on the incident or measurement directions, but it does depend on the wave number k. For our purpose this is good, since Saito's formula requires data over all directions at a high enough wave number. If one wants to use measurements at multiple frequencies, this approach is not so attractive due to the need to calculate a separate matrix for each wave number.

Remark 2.2. Multiple approaches to the numeric solution of the direct scattering problem exist, and we mention the volume integral equation methods, expanding grid methods and coupled finite element and boundary element methods (for more discussion see Section 8.7 of [3] and the references therein). The principal difficulty in all of the above methods is that the domain is infinite. Our approach is a modification of [31] and most akin to the integral equation method, where one solves the Lippmann-Schwinger equation directly. This strategy is well-suited to our purpose, since it is quite simple to compute the required integrals inside compact sets. Other methods are useful when one wants to know the solution to the scattering problem in large, possibly unbounded domains or if one wants to vary the wave number k.

Next, our task is to compute the scattering amplitude (6). Saito's formula asks for large k so we use a quadrature designed for oscillatory integrals. In [4] Evans and Webster propose a modified Levin method for the quadrature

$$I = \int_{-1}^{1} f(x)\mathrm{e}^{\mathrm{i}\tau x}\mathrm{d}x \approx \sum_{j=0}^{N} w_j f(x_j),$$

where the weights w_j are chosen so that the equation is exact for a set of functions f_k. Levin's approach is to pick $f_k = \mathrm{i}\tau p_k + p_k'$, $j = 0, \ldots, N$, in which case one obtains $N + 1$ complex linear equations

$$[p_k(x)\mathrm{e}^{\mathrm{i}\tau x}]_{-1}^{1} = \sum_{j=0}^{N} w_j \Big(\mathrm{i}\tau p_k(x_j) + p_k'(x_j)\Big).$$

At this point, Evans and Webster recommend the Chebyshev nodes $x_j = \cos(j\pi/N)$ and the Chebyshev polynomials $p_k(x) = T_k(x)$, $k = 0, \ldots, N$. We use $N = 13$. This choice leads to a stable (see page 210 of [4] for estimates) interpolatory quadrature rule which is exact for all polynomials of degree $\leq N$. This quadrature works on the interval $[-1, 1]$, but it is easy to deal with an arbitrary interval $[a, b]$ via the change of variables $x = \frac{1}{2}(b-a)t + \frac{1}{2}(b+a)$. The quadrature can also be implemented in the two-dimensional setting using formulae of Levin [20]. Figure 1 depicts the real-part of the scattering amplitude for incident direction $\theta = (1, 0) \in \mathbb{S}^1$ measured for fixed $k = 20$. In this example the potential function V is a characteristic function of a small ellipse, see Example 1 in Section 4.
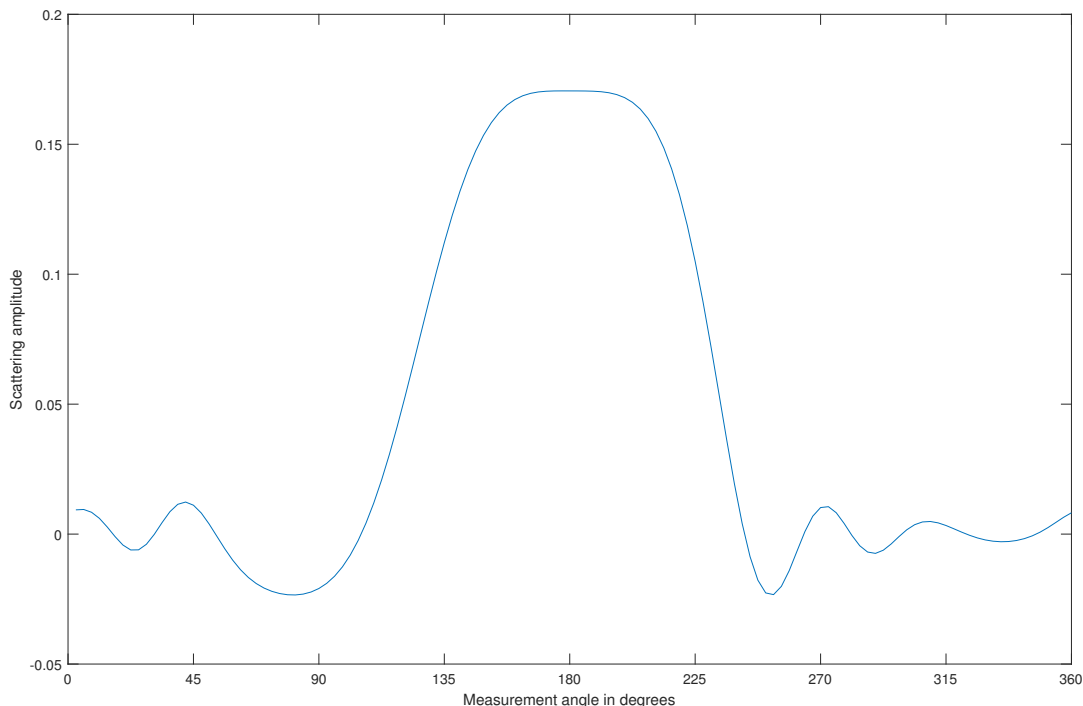
Figure 1: Real-part of the scattering amplitude with incident wave travelling to the right with direction $\theta = (1, 0)$ and $k = 20$. The potential is a characteristic function of an ellipse centered at $(1, 1)$.

3 Inverting Saito's formula

Having obtained the synthetic data $A(k, \theta, \theta')$ we can start working on the inverse problem. To use (5) one needs to calculate the double integral over the incident and

8

measurement directions. We do this via the usual polar coordinate expression

$$\int_{\mathbb{S}^1 \times \mathbb{S}^1} \mathrm{e}^{-\mathrm{i}k\langle\theta-\theta',\mathbf{x}\rangle} A(k,\theta,\theta')\mathrm{d}\theta\mathrm{d}\theta' = \int_0^{2\pi}\int_0^{2\pi} \mathrm{e}^{-\mathrm{i}k\langle\theta(t)-\theta'(s),\mathbf{x}\rangle} A(k,\theta(t),\theta'(s))\mathrm{d}t\mathrm{d}s,$$

(10)

where $\theta(t) := (\cos(t),\sin(t))$ and $\theta'(s) := (\cos(s),\sin(s))$. The double integral is calculated with Legendre-Gauss n-point quadrature rule.

Remark 3.1. The author also tested some quadratures designed for oscillatory integrals to integrate over the angles in Saito's formula, but these methods did not work so well. A possible alternative for Legendre-Gauss rule would be composite Simpson's quadrature, but in two dimensions this requires roughly four times the amount of incident and measurement directions only to result in similar accuracy. The reason is that n-point Simpson's rule (in one dimension) is accurate for polynomials of degree n, while Legendre-Gauss is exact for polynomials of order $2n$ (without subdivisions). Since the exponential in Saito's formula is oscillatory to some directions, the high order terms in its Taylor expansion will be significant. In possible applications Simpson's rule has the benefit that the nodes are evenly spaced. Some discussion on the difficulties arising from the kernels of the form $\exp(\mathrm{i}[x\cos(\theta) - y\sin(\theta)])$ for large $x,y \in \mathbb{R}$ can be found from [10].

Now (5) tells us that the above double integral at the limit $k \to +\infty$ is equal to

$$S(x) := 4\pi \int_{\mathbb{R}^2} \frac{V(\mathbf{y})}{|\mathbf{x} - \mathbf{y}|}\mathrm{d}\mathbf{y}.$$

This integral is of convolution type,

$$S(\mathbf{x}) = 4\pi \left(V * \frac{1}{|\cdot|}\right)(\mathbf{x}),$$

and it can be inverted by using techniques from harmonic analysis. Let us define the Fourier transform of a smooth rapidly decaying function f by

$$\widehat{f}(\xi) \equiv \mathcal{F}(f)(\xi) := \int_{\mathbb{R}^2} \mathrm{e}^{-2\pi\mathrm{i}\langle\mathbf{x},\xi\rangle} f(\mathbf{x})\mathrm{d}\mathbf{x}.$$

The inverse Fourier transform is given by

$$\mathcal{F}^{-1}(f)(\mathbf{x}) := \int_{\mathbb{R}^2} \mathrm{e}^{2\pi\mathrm{i}\langle\mathbf{x},\xi\rangle} f(\xi)\mathrm{d}\xi.$$

The Fourier transform can be extended to tempered distributions by duality. Let now $g(\mathbf{x}) = 1/|\mathbf{x}|$. It can be shown (see e.g., page 200 of [24]) that in the sense of tempered distributions

$$\mathcal{F}(g)(\xi) = \frac{1}{|\xi|}.$$

9

By using this, and the properties of the Fourier transform and convolution, we find the inversion algorithm

$$\frac{1}{4\pi}\mathcal{F}^{-1}\left(|\xi|\mathcal{F}\left(S\right)(\xi)\right)(\mathbf{x}) = \mathcal{F}^{-1}\left[|\xi|\mathcal{F}\left(V * \frac{1}{|\cdot|}\right)(\xi)\right](\mathbf{x})$$

$$= \mathcal{F}^{-1}\left(|\xi|\widehat{V}(\xi)\frac{1}{|\xi|}\right)(\mathbf{x})$$

$$= V(\mathbf{x}).$$

Actually, this theory is familiar from computed tomography, where in context of the X-ray transform it appears when working with the filtered back-projection (see for example [2]). The above high-pass filtering can be easily implemented numerically by using the fast Fourier transform. It should be noted that the choice of the filtering and the fast Fourier transform grid do affect the quality of the reconstruction.

Remark 3.2. In practise, instead of the high-pass filter $|\xi|$ one might use a different windowing function to enhance some desired features of the target. Some commonly used windowing functions are described in Section 7 of [2].

4 Examples

Let χ_A denote the characteristic function of a compact set $A \subset \mathbb{R}^2$ as in (9) and let $\varphi_A \in C_0^\infty(\mathbb{R}^2)$ be a smooth function, supported in A. More precisely, the φ_A-function we use is given as a C_0^∞-function on an ellipse $\{(x, y) \in \mathbb{R}^2 \mid (x/a)^2 + (y/b)^2 < 1, a, b > 0\}$ by the formula

$$\varphi_{\text{ellipse}}(x, y) = \begin{cases} \exp\left(\frac{1}{(x/a)^2 + (y/b)^2 - 1}\right), & (x/a)^2 + (y/b)^2 < 1, \\ 0, & \text{otherwise.} \end{cases}$$

We also apply a rotation, so that the ellipse is tilted by 45 degrees. In the sequel we consider the following examples:

1. $V(\mathbf{x}) = 0.5\chi_{\text{ellipse}}(\mathbf{x})$, for $k = 5, 10, 14, 15, 20, 25$,

2. $V(\mathbf{x}) = 0.5\chi_{\text{rectangle}}(\mathbf{x})$, for $k = 20$,

3. $V(\mathbf{x}) = 0.25\varphi_{\text{ellipse}}(\mathbf{x})$, for $k = 10$,

4. $V(\mathbf{x}) = 0.5\chi_{\text{U}}(\mathbf{x})$, for $k = 10$.

5. $V(\mathbf{x}) = 0.5\chi_{\text{square}}(\mathbf{x}) + 0.7\chi_{\text{ellipse}}(\mathbf{x})$, for $k = 30$.

In all of the examples the data $A(k, \theta, \theta')$ is corrupted by Gaussian white noise with standard deviation $\sigma = 0.02 \max(|A(k, \theta, \theta')|)$. The measurements are conducted at 64 incident and 64 measurement angles, determined by the Legendre-Gauss quadrature nodes (see (10)), yielding a total of 4098 measurements. The support of V is divided into 6400 pixels and the construction of the 6400×6400-matrix $\mathcal{L}$ is done in 12 minutes. The evaluation of the solution u with five iterations of the Neumann series combined with the computation of the oscillatory Fourier integral at 4098 points takes approximately 14 minutes on a standard desktop computer with an Intel i7 processor and 16 Gb RAM. Computation of both could possibly be optimized further by better employing parallel computation.

Given the measurements the inversion algorithm is fast. Let $Q = [-4, 4] \times [-4, 4]$ be the reconstruction grid, which contains the support of the unknown potential V. We divide the reconstruction grid into $80 \times 80 = 6400$ evenly sized pixels. The numeric integration with Legendre-Gauss rule is simply a sum of 4098 elements at each of the 6400 pixels and can be done in 1–1.5 seconds. The high-pass filtering with fast Fourier transform is equally quick, happening almost instantaneously. Figure 2 shows the double integral of (5) (the left-hand side) computed from the synthetic measurement and the precise convolution integral computed using the actual unknown for Example 1. The resulting reconstructions from the high-pass filtering are depicted in Figures 3–9, where the figure on the left shows the precise unknown and the figure on the right is the numerically computed reconstruction from synthetic measurements. The relative errors

$$\varepsilon_{\mathrm{rel}} = \frac{|V(\mathbf{x}) - \widetilde{V}(\mathbf{x})|}{\|V\|_{L^\infty(\mathbb{R}^2)}}$$

of Example 1 are shown in Figure 5. Here $\widetilde{V}$ denotes the numerical reconstruction.

5   Conclusions

We described an approach to implementing Y. Saito's formula from 1982 numerically. As it turns out, one has to be little careful when generating synthetic data in the presence of multiple oscillatory integrals. The difficulties with oscillations can be overcome by separating the region of integration into smaller pixels and using quadratures designed for oscillatory integrals. The inversion of Saito's formula is done at a fixed wave number k by numerically integrating with Legendre-Gauss quadrature and then deblurring the result with the fast Fourier transform and a high-pass filter. The resulting reconstructions indicate that this method can be used to recover important information (shape, location and to a reasonable extent size) about the potential function.
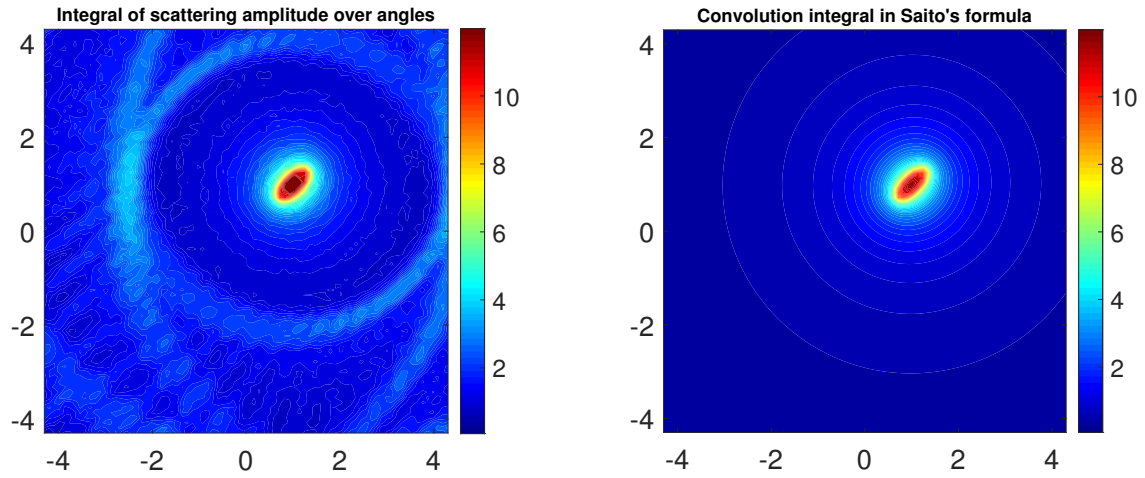
Figure 2: Example 1. The result of the integral of the scattering amplitude over directions on the right compared to the precise convolution integral of the unknown potential on the left.
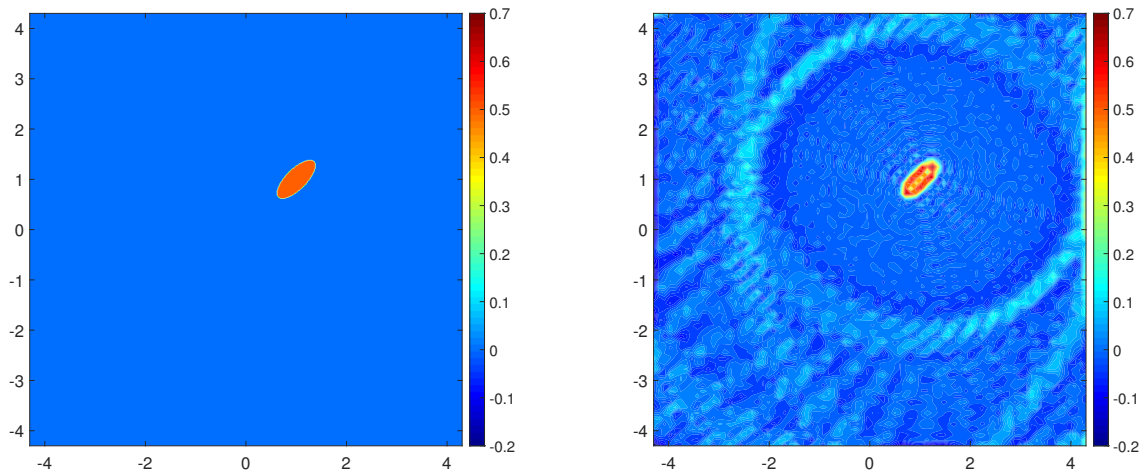

Figure 3: Far-view of Example 1 with $k = 14$. Precise unknown on the left and the numeric reconstruction on the right. Some error can be seen further away from the potential V. This is caused by the number of Legendre-Gauss quadrature nodes in the integration of Saito's formula. Location and shape of the scatterer are captured quite accurately.
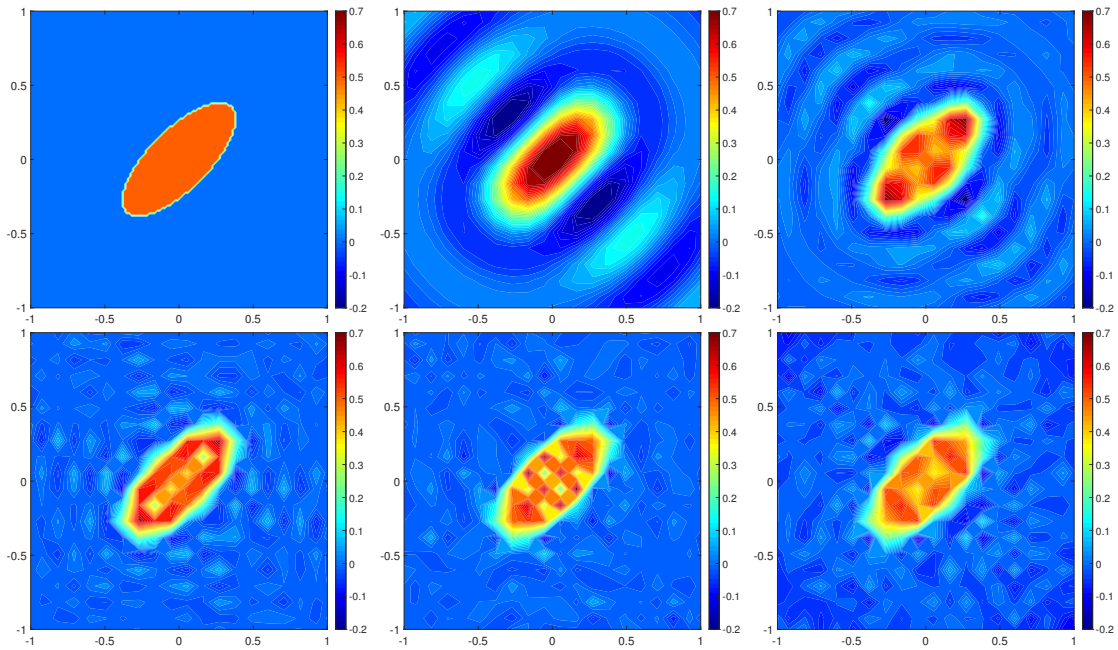
Figure 4: Example 1. Comparison of different values $k = 5$ top-middle, $k = 10$ top-right, $k = 15$ bottom-left, $k = 20$ bottom-middle and $k = 25$ bottom-right. Top-left figure is the precise unknown target.

13
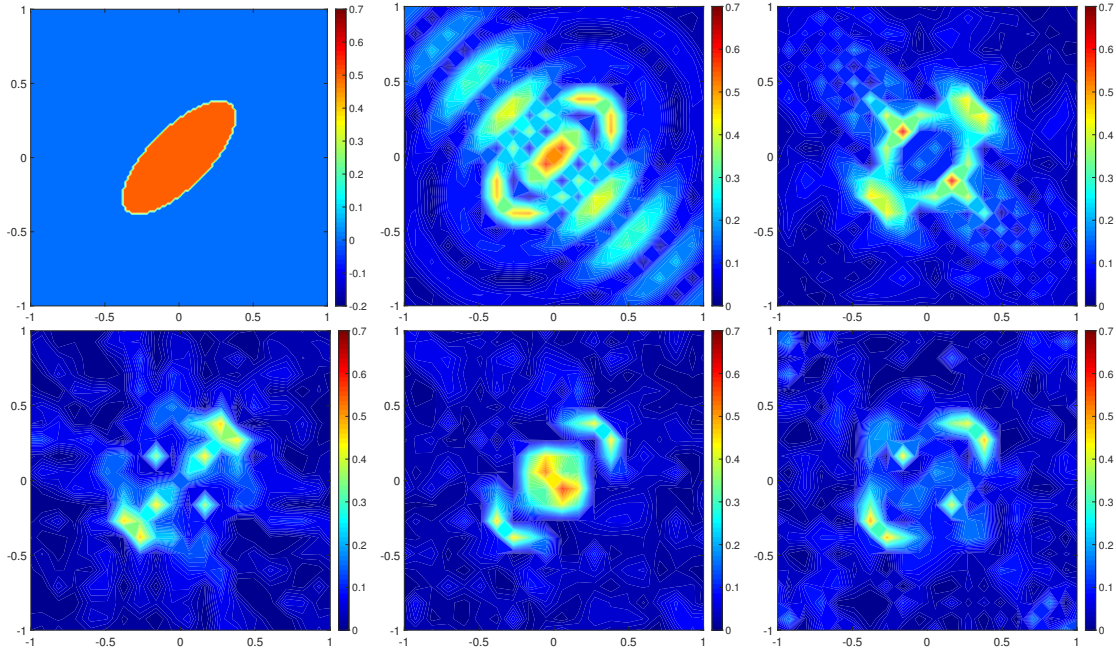
Figure 5: Example 1. Comparison of the relative errors at different values $k = 5$ top-middle, $k = 10$ top-right, $k = 15$ bottom-left, $k = 20$ bottom-middle and $k = 25$ bottom-right. Top-left figure is the precise unknown target. Some error can be seen at the boundary of the characteristic function (jump discontinuity) for the values $k = 10, 15, 25$ while there is also some error in the middle when $k = 5, 20$.
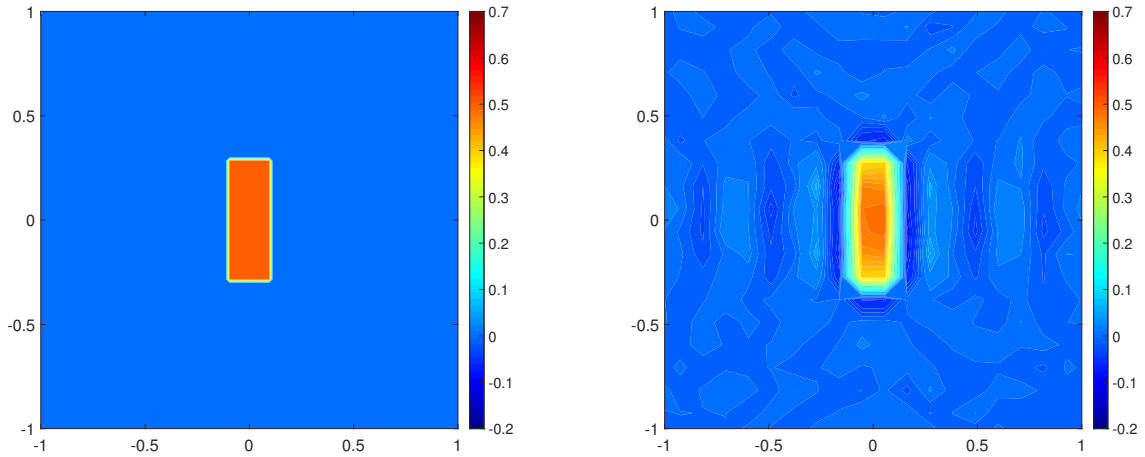
Figure 6: Example 2 with $k = 20$. The target is a characteristic function of a rectangle. Precise unknown on the left and the numeric reconstruction on the right.
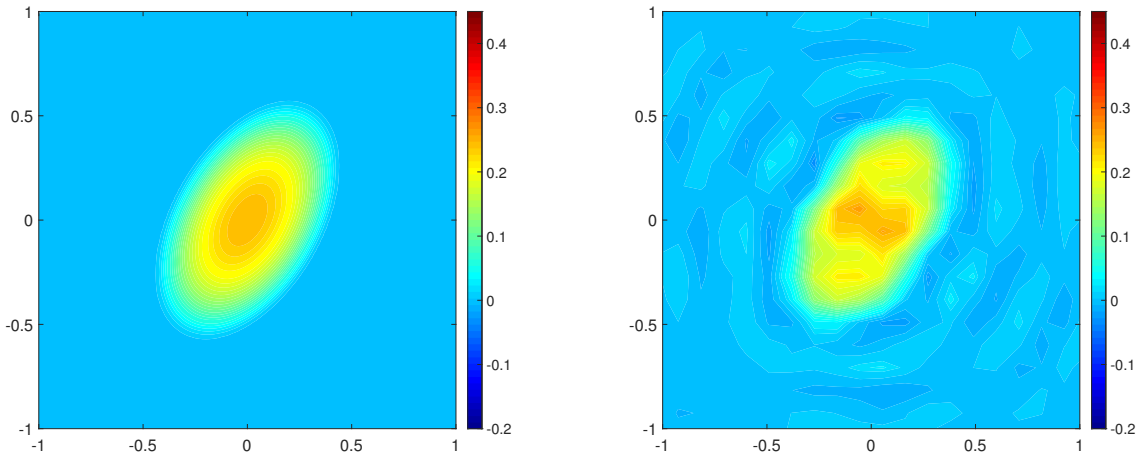
Figure 7: Example 3 with $k = 10$. The target is a smooth bump function supported in an ellipse. Precise unknown on the left and the numeric reconstruction on the right.
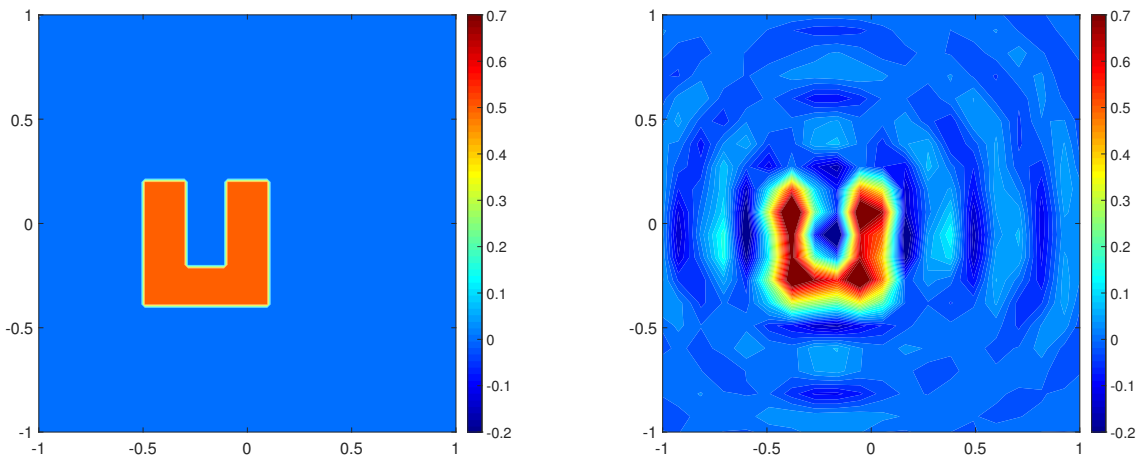

Figure 8: Example 4 with $k = 10$. The target is a characteristic function of a U-shaped region. Precise unknown on the left and the numeric reconstruction on the right.

15

Acknowledgement

References

[1] S. Agmon. Spectral properties of Schrödinger operators and scattering theory. *Ann. Scuola Norm. Sup. Pisa*, 2:151–218, 1975.

[2] T.M. Buzug. *Computed Tomography: From Photon Statistics to Modern Cone-Beam CT*. Springer, Berlin Heidelberg, 2008.

[3] D. Colton and R. Kress. *Inverse acoustic and electromagnetic scattering theory*. Springer, New York, 2010.

[4] G.A. Evans and J.R. Webster. A high order, progressive method for the evaluation of irregular oscillatory integrals. *Appl. Num. Math.*, 23:205–218, 1997.

[5] G.A. Evans and J.R. Webster. A comparison of some methods for the evaluation of highly oscillatory integrals. *J. Comp. Appl. Math.*, 112:55–69, 1999.

[6] G. Fotopoulos and M. Harju. Inverse scattering with fixed observation angle data in 2D. *Inv. Prob. Sci. Eng.*, 25:1492–1507, 2017.

[7] G. Fotopoulos, M. Harju, and V. Serov. Inverse fixed angle scattering and backscattering for a nonlinear Schrödinger equation in 2D. *Inverse Prob. Imag.*, 7:183–197, 2013.

[8] G. Fotopoulos and V. Serov. Inverse fixed energy scattering problem for the two-dimensional nonlinear Schrödinger operator. *Inverse Probl. Sci. Eng.*, 24:692–710, 2016.

[9] M. Harju. Numerical computation of the inverse Born approximation for the nonlinear Schrödinger equation in two dimensions. *Comput. Methods Appl. Math.*, 16:133–143, 2016.

[10] D. R. Hartree. The evaluation of a diffraction integral. *Math. Proc. Cambridge*, 50(4):567–574, 1954.

[11] M.V. de Hoop, M. Lassas, M. Santacesaria, S. Siltanen, and J.P. Tamminen. Positive-energy D-bar method for acoustic tomography: a computational study. *Inverse problems*, 32:025003, 2016.

[12] A. Iserles. On the numerical quadrature of highly-oscillating integrals I: Fourier transforms. *IMA J. Num. Anal.*, 24:365–391, 2004.

[13] A. Iserles. On the numerical quadrature of highly-oscillating integrals II: Irregular oscillators. *IMA J. Num. Anal.*, 25:25–44, 2004.

[14] H. Isozaki. *Maxwell equation: inverse scattering in electromagnetism*. World Scientific Publishing Co. Pte. Ltd., 2018.

[15] M.V. Klibanov. Convexification of restricted Dirichlet-to-Neumann map. *J. Inverse and Ill-Posed Problems*, 25:669–685, 2017.

[16] M.V. Klibanov, A.E. Kolesov, and D.-L. Ngueyen. Convexification method for an inverse scattering problem and its performance for experimental backscatter data for buried targets. *SIAM J. Imaging Sciences*, 12:576–603, 2019.

[17] M.V. Klibanov, J. Li, and W. Zhang. Convexification of electrical impedance tomography with restricted Dirichlet-to-Neumann map data. *Inverse problems*, 35:35005, 2019.

[18] R. Kress. A Nyström method for boundary integral equations in domains with corners. *Numer. Math.*, 58:145–161, 1990.

[19] R. Kress. *Numerical analysis*. Springer, New York, 1998.

[20] D. Levin. Procedures for computing one- and two-dimensional integrals of functions with rapid irregular oscillations. *Math. Comp.*, 32(158):531–538, 1982.

[21] L. Päivärinta and V. Serov. Recovery of singularities of a multidimensional scattering potential. *SIAM J. Math. Anal.*, 29:697–711, 1998.

[22] Y. Saitō. Some properties of the scattering amplitude and the inverse scattering problem. *Osaka J. Math.*, 19:527–547, 1982.

[23] V. Serov. Inverse fixed angle scattering and backscattering problems in two dimensions. *Inverse Problems*, 24(6):065002, 2008.

[24] V. Serov. *Fourier series, Fourier transform and their applications to mathematical physics*. Springer, 2017.

[25] V. Serov, G. Fotopoulos, and M. Harju. Direct and inverse scattering for nonlinear Schrödinger equation in 2D. *J. Math. Phys.*, 53:123522, 2012.

[26] V. Serov, M. Harju, and G. Fotopoulos. Some recent advances in nonlinear inverse scattering in 2D: theory and numerics. *Appeared in Applied Linear Algebra in Action (Intech, Croatia)*, pages 115–137.

[27] L.F. Shampine. Efficient Filon method for oscillatory integrals. *Appl. Math. Comp.*, 221:691–702, 2013.

[28] A. Sommerfeld. *Partial differential equations in physics*. Academic Press, New York, 1949.

[29] T. Tyni and M. Harju. Inverse backscattering problem for perturbations of biharmonic operator. *Inverse Problems*, 33:105002, 2017.

[30] T. Tyni and V. Serov. Scattering problems for perturbations of the multidimensional biharmonic operator. *Inverse Prob. Imag.*, 12(1):205–227, 2018.

[31] G. Vainikko. Fast solvers of the Lippmann-Schwinger equation. *In: Gilbert R.P., Kajiwara J., Xu Y.S. (eds) Direct and Inverse Problems of Mathematical Physics. International Society for Analysis, Applications and Computation*, 5:423–440, 2000.
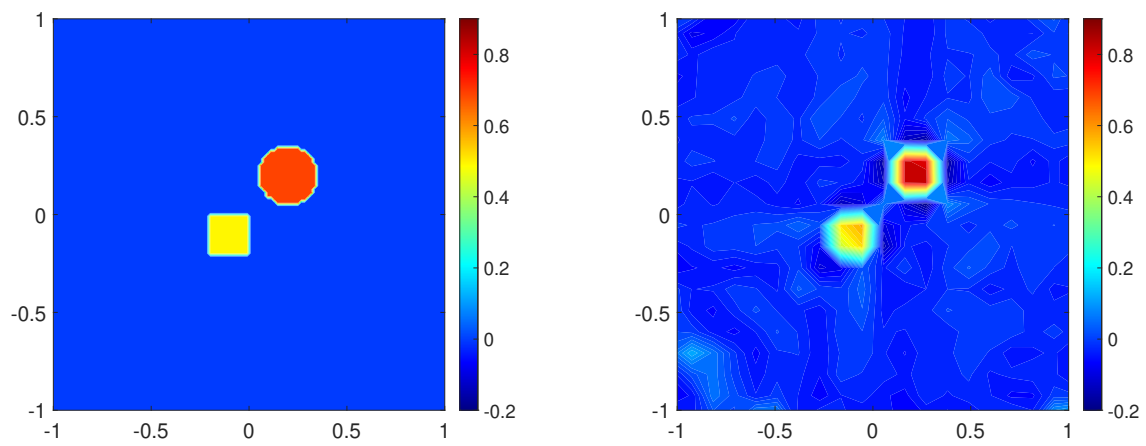
Figure 9: Example 5 with $k = 30$. The support of the target is non-connected, constisting of characteristic functions of a disc and a square. Precise unknown on the left and the numeric reconstruction on the right.